Magnetic Devices for Ultra High Throughput Biological Analysis

T. Mitrelias, Z. Jiang, J. Llandro and J.A.C. Bland

Cavendish Laboratory, University of Cambridge, JJ Thomson Avenue,
Cambridge CB3 0HE, United Kingdom, tm10007@cam.ac.uk

ABSTRACT

We have developed a magnetic biosensor based on a lab-on-a-chip integrated microfluidic cell for detection and sorting of magnetic microbeads in solution comprising magnetoresistive sensors and tapered current carrying striplines integrated with a microfluidic channel. The suspended beads are moved along a microfluidic channel patterned in SU8 over 10 μm diameter ring shaped sensors arranged in Wheatstone bridge. The device reads the real-time voltage signal as a bead perturbs an in-plane applied field in the vicinity of the active bridge elements. Beads of different magnetic moments can be detected and sorted through a magnetostatic sorting gate into different branches of the microchannel. The cell is unique because its design facilitates the integration of magnetic sensors with microfluidics and because it has individually addressable sorting striplines that divert magnetic beads in flow by applying currents locally as opposed to globally applied fields that are used to divert beads in non-flowing mode.

Keywords: magnetic biosensors, magnetic beads, microfluidics

1 INTRODUCTION

In the past few years there has been a considerable effort to develop appropriate techniques and devices to address the need for fast, reliable, low cost, high throughput bioassays. One of the main aims of this research effort is to develop biosensors that can detect a large number of pathogens in a single test in a highly parallel fashion. The physical principle on which the operation of these biosensors is based is molecular recognition, i.e. the ability of a known compound (probe) to specifically identify and hybridize with its exact complementary compound (target), if the later is present in a sample. The state of the art systems for high throughput biological analysis are microarrays that employ fluorescence labeling, but have inherent low sensitivity due to the fact that they require 10^4 molecules to achieve good signal to noise ratio [1]. Magnetic lab-on-chip diagnostic devices have been proposed for the screening of biological samples and the detection of pathogens that are present at low concentrations in a biological sample. The development of novel magnetic biosensors that utilize magnetic microbeads functionalized with biological molecules has attracted considerable interest [2], since they offer some unique advantages, such as highly sensitive and rapid detection, low cost and the ability to integrate with conventional electronic circuits. A further advantage of magnetic sensors as compared to conventional biosensors based on optical detection is their ability to be easily miniaturized due to the electronic nature of the detected signal. Additionally, no optics setup is required and the background signals are extremely low since biological fluids are not magnetic while they tend to exhibit autofluorescence.

Detection of a magnetic microbead signifies the presence or absence of the particular biomolecule attached to the bead in the sample. However, an ideal magnetic device for efficient high throughput biological analysis must be able to detect single magnetic functionalized beads, a requirement that necessitates the use of advanced magnetic sensors. Magnetic sensors based on the magnetoresistance (MR) effect have been used as detection elements for biochips that utilize magnetic beads as labels [3, 4, 5]. Several sensors geometries have been proposed, such as single anisotropic magnetoresistive (AMR) rings [6], Hall crosses [7], spin valve rectangles [8] and magnetic tunnel junctions ellipses [9].

In addition to sensitive detection elements, a magnetic device developed for practical immunoassay applications and high throughput analysis must integrate microfluidic channels for the beads to flow through, as well as systems to manipulate the microbeads together with the sensing elements and external fluidic connections. Several different strategies for bead manipulation and sorting have been investigated, usually involving local magnetic field gradients generated by microelectromagnets acting on beads or stationary suspensions [10]. We have developed an Integrated Microfluidic Cell (IMC) comprising three types of MR sensors, focusing electrodes, a sorting gate and tapered current lines integrated with a microfluidic channel for the focusing, sorting and detection of single magnetic functionalized microbeads in solution.

2 RESULTS AND DISCUSSION

The IMC device was fabricated on an undoped 15x20 mm GaAs substrate by patterning in a double layer photoresist combination of 5.5 μm thick SPR220-7 on top of 4 μm thick LOR 30B lift-off promoter, followed by thermal evaporation of Cr(2 nm)/$Ni_{30}Fe_{70}$(34 nm)/Cr(2 nm) in an Edwards evaporator at a pressure of $2x10^{-6}$ mbar. A film of Cr(2 nm)/Cu(120 nm)/Cr(2 nm) was then evaporated and patterned by lift-off of another SPR220-7/LOR 30B resist template to form the sensor contacts and manipulation striplines. The entire area was covered by a layer of 400 nm thick SU8 2000.5 photoresist for protection and insulation of the chip. A 75 μm wide and 75 μm deep microchannel was subsequently defined by standard optical lithography in SU8 2100. The device, shown in Figure 1, was finally completed by sealing the channel with a 2 mm thick lid stamped from a film of polydimethysiloxane (PDMS). Freshly cured PDMS film forms a good conformal seal with newly developed SU8 under light compression. Fluidic connections are made by inserting 2 mm PTFE tubes into freshly-punched circular holes in the lid.

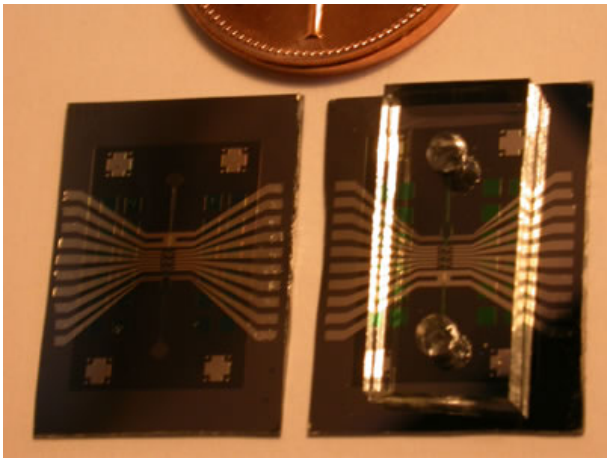

Figure 1: A photograph of the IMC showing the device without and with the PDMS lid on the left and right respectively.

2.1 Magnetic Sensors

The detection of a single magnetic bead is based on the detection of magnetic field changes that result from the dipole field produced by the bead that opposes and partially cancels an in-plane applied sensor field. The dipole field $H_x(z)$ (in plane component) produced by a magnetic bead with moment m_b [7] at a distance z in an area of the order of the bead crossection directly below the bead is

$$H_x(z) \approx \frac{-0.38 m_b}{4\pi z^3} \quad (1)$$

In our experiments the distance z is the sum of the radius of the bead and the thickness of the insulation layer of the device. To optimize the detection, a sensor with dimensions similar to the bead being detected must be designed and in addition, the sensor-bead distance must be minimized. Hence, it is necessary to design an advanced bead manipulation system that can be used to precisely transport the beads and position them directly on top of the magnetic sensors. Moreover, the sensor must have sufficient sensitivity (ΔR/R vs. H) to provide a response to the dipole field of the bead H with high signal to noise ratio.

Mesoscopic AMR rings have been selected as the most appropriate sensors for single bead detection, since they offer good matching intrinsically with the magnetic flux pattern from a magnetic bead [3]. The reversal characteristics of ring sensors have been previously studied and reproducible switching between well defined high magnetization (onion) and zero magnetization (vortex) states under an external field of several hundreds of Oe has been shown [11]. The presence of a bead will prevent the switching of the ring sensors and provide a detection signal when a DC in-plane bias field is applied to keep the ring close to its switching point. To further enhance the signal to noise ratio, the sensors have been arranged in a constant current driven Wheatstone bridge configuration with two active sensors and two reference sensors in opposite arms of the bridge. External interference is thus minimized and, in addition, the output signal is doubled.

Figure 2(a) shows three types of sensors fabricated by MBE growth for the IMC: AMR rings of 6 μm inner diameter and 10 μm outer diameter are shown in Figure 2(d) and 18x4.5 μm rectangular sensors with their long axes parallel and perpendicular to the channel direction are shown in Figures 2(e) and 2(f) respectively. The focusing electrodes are placed at one end of the sensor array to focus the magnetic beads into the central gap between them, as shown in Figure 2(b). The beads subsequently move along the central microchannel to pass over the sensors. The focusing striplines have been designed with an appropriate shape to provide a uniform field gradient of 0.08 T/m (for a DC current of 0.2 A) along the central line of the channel. In addition, we have used a y-shaped microfluidic channel flanked by independently powered tapered current striplines to generate the local fields necessary for bead sorting, as shown in Figure 2(c). Each pair of the sorting striplines can be independently switched to produce the magnetic field gradient and thus attract passing beads into its associated branch.

To demonstrate the sensitivity of the detector bridge, the voltage output of the AMR ring bridge was measured in response to applied field strengths comparable to those generated by a ferromagnetic bead in close proximity to the sensor. The beads that were used in this study were commercially available Spherotech CFM-80-5 ferromagnetic 8.92 μm in diameter. The MR response curve of the rings under ±200 Oe applied in-plane field along the channel direction is shown in Figure 3, with the two outer rings magnetically shielded for the purpose of this experiment. A linear response in the range 22-77 Oe is observed with an output ratio of 0.25% that corresponds to an AMR ratio of 0.5% for each ring. With only two equatorial contacts to each ring, the two high field magnetic states of the ring give the same ΔR, resulting in a symmetrical output curve. When a biasing field of 80 Oe is applied to the bridge, the magnetic moment of the beads is approximately $1x10^{-8}$ emu. From equation (1) we calculate that 9 μm beads produce a field of H = 35 Oe at a bead-sensor distance of 4.9 μm (i.e. when the bead is in contact with the sensor, taking into account the thickness of the insulation layer). From the MR transfer curve we can thus deduce that this is a field sufficient to generate a measurable change in the signal level from the bridge.

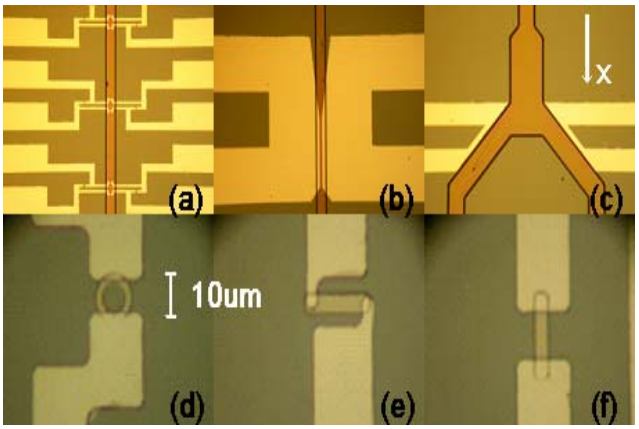

Figure 2: (a) Sensor bridges in the microchannel; (b) focusing electrodes; (c) sorting gate; (d), (e) and (f) ring and block sensors.

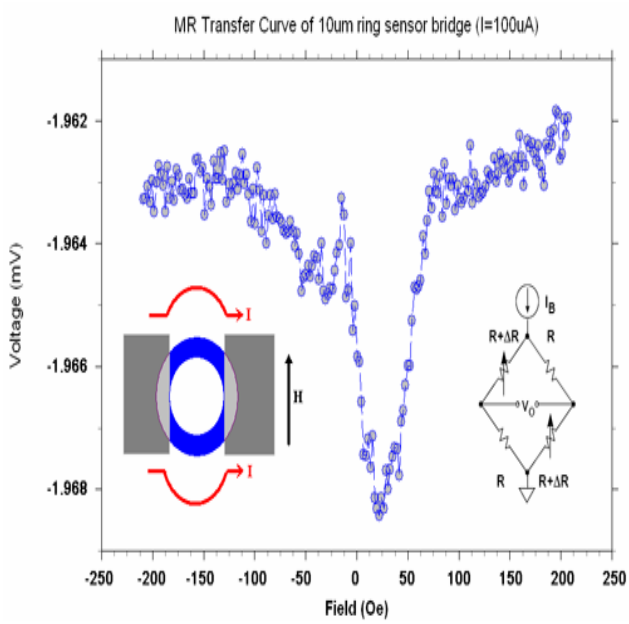

Figure 3: MR transfer curve of AMR sensor bridge for 100 μA biasing current.

2.2 Manipulation and Sorting Systems

Bead sorting and magnetic field induced manipulation has also been demonstrated using the sorting gate and the focusing electrodes of the IMC and presented in Figure 4. Ferromagnetic beads are flowing down the channel under the influence of gravity and capillary forces when the IMC device is inclined several tens of degrees from the horizontal level. When no current is applied the beads flow equally down both branches of the y-shaped gate [Figure 4(a)]. Figure 4(b) show beads flowing down the left channel when a 0.2 A DC current is applied to the left stripline only. The beads begin to be attracted towards the stripline at a distance of about 210 μm from the top corner of the stripline (marked A in the figure). The maximum velocity a bead can reach for a given current at each point along the flow direction, occurs when the magnetic attraction force balances the drag force. This velocity can be obtained by equating the viscous drag on a sphere in suspension and the Biot-Savart attraction from a wide current-carrying stripline of infinite length [12]:

$$\left(\frac{dx}{dt}\right)_{crit} = \frac{V\chi\mu^2 \ln\left(\frac{x}{x+b}\right)}{4\mu_0\pi^2 bx(x+b)(3\pi\eta a)} I^2 \qquad (2)$$

The critical velocity decreases with the distance to the stripline. A bead will begin to be attracted only when this velocity overcomes its Brownian drift velocity, that is about 0.3 μm/s for 9 μm beads suspended in water. Substituting into equation (2), we calculate that the stripline will attract

beads within a distance of 215 μm when powered by a DC current of 0.2 A, a value that agrees very well with the experimental data.

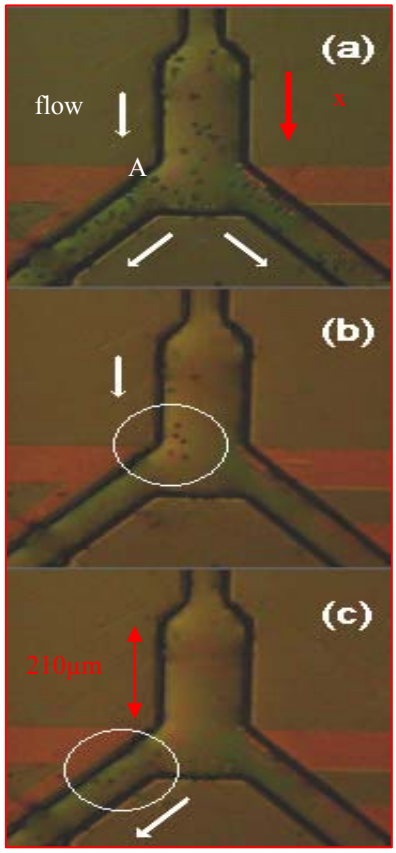

Figure 4: Ferromagnetic beads flowing through the sorting gate.

3 CONLCUSIONS

An Integrated Microfluidic Cell (IMC) designed for the detection of biological compounds attached to magnetic beads has been fabricated and successfully tested. The IMC device comprises magnetic sensors and current carrying striplines for the manipulation, sorting and detection of the beads. The MR response curve of the detector bridge has been measured and shows that the rings have an AMR ratio of 0.5% with a linear response between 22 and 77 Oe and it is concluded that the sensor bridge is capable of detecting single 9 μm ferromagnetic beads with high signal to noise ratio at a distance of 4.7 μm from the surface of the active sensor. This can be achieved by manipulating the beads and positioning them directly on top of the sensor. We have demonstrated that the beads can flow through the microchannel and can be manipulated by the magnetic field gradients generated by the sorting striplines at a distance of up to 200 μm. We therefore conclude that the viability of this design for detection and sorting of single magnetic beads has been demonstrated.

We are planning to extend these experiments and we have already fabricated a next generation IMC device with sensors comprising giant magnetoresistive (GMR) elements that should provide higher signal sensitivity [13, 14]. The device is currently being tested and the first results will be reported in the near future. Our ultimate aim is to design similar lab-on-a-chip devices to perform ultra high throughput biological assays utilizing the magnetic characteristics of different magnetic particles. The particles will be used as labels for tagging various biological compounds that can be manipulated, sorted and detected in a single assay in a highly parallel fashion. We are also planning to carry out experiments for human cells separation and detection using ferromagnetic beads with different magnetic moments that can be used to uniquely identify different species attached to them.

REFERENCES

[1] M. Shena and R.W. Davis, *Microarray Biochip Technology*, Eaton Publishing, pp 1-18 (2000)

[2] M. Megens and M. Prins, *J. Magn. Mag. Mat.* **293**, 702 (2005)

[3] D.R. Baselt, G.U. Lee, M. Natesan, S.W. Metzger, P.E. Sheehan and R.J. Colton, *Biosens. and Bioelectr.* **13** 731 (1998)

[4] S.X. Wang, S-Y. Bae, G. Li, S. Sun, R.L. White, J.T. Kemp, C.D. Webb, *J. Magn. Magn. Mat.*, **293** 731 (2005)

[5] M. Brzeska, M. Panhorst, P.B. Kamp, J. Schotter, G. Reiss, A. Puhler, A. Becker and H. Bruckl, *J. Biotechn.* **112** 25 (2004)

[6] M.M. Miller, G.A. Prinz, S-F. Cheng, and S. Bounnak, *Appl. Phys. Lett.* **81** 2211 (2002)

[7] L. Ejsing, M.F. Hansen, A.K. Menon, H.A. Ferreira D.L. Graham and P.P. Freitas, *J. Magn. Magn. Mat.* **293** 677 (2005)

[8] H.A. Ferreira, D.L. Graham, P.P. Freitas and J.M.S Cabral, *J. Appl. Phys.* **93(10)** 7281 (2003)

[9] W. Shen, X. Liu, D. Mazumdar and G. Xiao, *Appl. Phys. Lett.*, **86**, 253901 (2005)

[10] L. Lagae, r. Wirix-Speetjens, J. Das, D. Graham, H. Ferreira, P.P. Freitas, G. Borghs and J. de Boeck, *J. Appl. Phys.*, **91(10)** 7445 (2002)

[11] M. Klaui, C.A.F. Vaz, J.A.C. Bland, W. Wernsdorfer, G. Faini and E. Cambril, *J. Appl. Phys.* **93(10)** 7885 (2003)

[12] N. Pekas, M. Granger, M. Tondra, A. Popple and M.D. Porter, *J. Magn. Magn. Mater.* **293** 584 (2005)

[13] Z. Jiang, J. LLandro, T. Mitrelias and J.A.C. Bland *J. Appl. Phys.*, in press

[14] J, Llandro, Z. Jiang, T. Hayward, T. Mitrelias and J.A.C. Bland, to be published